Birefringent in-phase supermode operation of a multicore microstructured fiber laser

X. Zhu, A. Schülzgen, L. Li, H. Li, V. L. Temyanko, J. V. Moloney, and N. Peyghambarian

College of Optical Sciences, University of Arizona, 1641 East University Boulvard, Tucson, Arizona 85721, USA
xszhu@email.arizona.edu

Abstract: We report the first observation of birefringent in-phase supermode operation of a phase-locked multicore fiber laser. The in-phase mode operation of our 12-core rectangular-array microstructured fiber laser was confirmed by the near-field distribution, the far-field diffraction pattern, and the optical spectrum. The birefringence of the in-phase mode in propagation constant $\Delta\gamma$ was measured as $\sim 4 \times 10^{-6}$ 1/μm. The break of the polarization degeneracy indicates the possibility of single polarization operation of phase-locked multicore fiber lasers and amplifiers.

OCIS codes: (140.3290) Laser arrays; (140.3510) Fiber lasers; (260.1440) Birefringence; (060.2280) Fiber design and fabrication.

References and links

1. D. R. Scifres, R. D. Burnham, and W. Streifer, "Phase-locked semiconductor laser array," Appl. Phys. Lett. **32**, 1015-1017 (1978).
2. M. Oka, H. Masuda, Y. Kaneda, and S. Kubota, "Laser-diode-pumped phase-locked Nd:YAG laser arrays," IEEE J. Quantum Electron. **28**, 1142-1147 (1992).
3. D. G. Youmans, "Phase locking of adjacent channel leaky waveguide CO_2 lasers," Appl. Phys. Lett. **44**, 365-367 (1984).
4. J. Morel, A. Woodtli, and R. Dandliker, "Coherent coupling of an array of Nd^{3+}-doped single-mode fiber lasers by use of an intracavity phase grating," Opt. Lett. **18**, 1520-1522 (1993).
5. Y. Jeong, J. K. Sahu, D. Payne, and J. Nilsson, "Ytterbium-doped large-core fiber laser with 1.36 kW continuous-wave output power," Opt. Express **12**, 6088-6092 (2004).
6. T. Qiu, L. Li, A. Schülzgen, V. Temyanko, T. Luo, S. Jiang, A. Mafi, J. Moloney, N. Peyghambarian, "Generation of 6.6 W multimode and 4 W single mode output from 7 cm short fiber lasers," IEEE Photon. Technol. Lett. **16**, 2592-2594 (2004).
7. T. Qiu, S. Suzuki, A. Schülzgen, L. Li, A. Polynkin, V. Temyanko, J. Moloney, and N. Peyghambarian, "Generation of watts-level single-longitudinal-mode output from cladding-pumped short fiber lasers," Opt. Lett. **30**, 2748-2750 (2005).
8. X. Zhu and R. K. Jain, "10-W-level diode-pumped compact 2.78 μm ZBLAN fiber laser," Opt. Lett. **32**, 26-28 (2007).
9. D. R. Scifres, "Multiple core fiber lasers and optical amplifiers," US Patent #5,566,196 (1996).
10. M. Wrage, P. Glas, D. Fischer, M. Leitner, D. V. Vysotsky, and A. P. Napartovich, "Phase locking in a multicore fiber laser by means of a Talbot resonator," Opt. Lett. **25**, 1436-1438 (2000).
11. M. Wrage, P. Glas, and M. Leitner, "Combined phase locking and beam shaping of a multicore fiber laser by structured mirrors," Opt. Lett. **26**, 980-982 (2001).
12. M. Wrage, P. Glas, D. Fischer, M. Leitner, N. N. Elkin, D. V. Vysotsky, A. P. Napartovich, and V. N. Troshchieva, "Phase-locking of a multicore fiber laser by wave propagating through an annular waveguide," Opt. Commun. **205**, 367-375 (2002).
13. L. Michaille, C. R. Bennett, D. M. Taylor, T. J. Shepherd, J. Broeng, H. R. Simonsen, and A. Peterson, "Phase locking and supermode selection in multicore photonic crystal fiber lasers with a large doped area," Opt. Lett. **30**, 1668-1670 (2005).
14. P. K. Cheo, A. Liu, and G. G. King, "A high-brightness laser beam from a phase-locked multicore Yb-doped fiber laser array," IEEE Photon. Technol. Lett. **13**, 439-441 (2001).
15. L. Li, A. Schülzgen, S. Chen, V. L. Temyanko, J. V. Moloney, and N. Peyghambarian, "Phase locking and in-phase supermode selection in monolithic multicore fiber lasers," Opt. Lett. **31**, 2577-2579 (2006).

#83153 - $15.00 USD Received 16 May 2007; revised 27 Jul 2007; accepted 30 Jul 2007; published 1 Aug 2007

16. R. J. Beach, M. D. Feit, S. C. Mitchell, K. P. Cutter, S. A. Payne, R. W. Mead, J. S. Hayden, D. Krashkevich, and D. A. Alumni, "Phase-locked antiguided multiple-core ribbon fiber," IEEE Photon. Technol. Lett. **15**, 670-672 (2003).
17. J. Yoo, J. R. Hayes, E. G. Paek, A. Scherer, and Y. Kwon, "Array mode analysis of two-dimensional phased arrays of vertical cavity surface emitting lasers," IEEE J. Quantum. Electron. **26**, 1039-1051 (1990).
18. J. C. Knight, T. A. Birks, P. St. J. Russell, and D. M. Atkin, "All-silica single-mode optical fiber with photonic crystal cladding," Opt. Lett. **21**, 1547-1549 (1996).
19. R. F. Cregan, B. J. Mangan, J. C. Knight, T. A. Birks, P. St. J. Russell, P. J. Roberts, D. C. Allan, "Single-mode photonic band gap guidance of light in air," Science **285**, 1537-1539 (1999).
20. J. K. Ranka, R. S. Windeler, and A. J. Stentz, "Visible continuum generation in air-silica microstructure optical fibers with anomalous dispersion at 800 nm," Opt. Lett. **25**, 25-27 (2000).
21. H. Kubota, S. Kawanishi, S. Koyanagi, M. Tanaka, and S. Yamaguchi, "Absolutely single polarization photonic crystal fiber," IEEE Photon. Technol. Lett. **16**, 182-184 (2004).
22. A. Mafi and J. V. Moloney, "Shaping modes in multicore photonic crystal fibers," IEEE Photon. Technol. Lett. **17**, 348-350 (2005).
23. J. K. Butler, D. E. Ackley, and D. Botez, "Coupled-mode analysis of phase-locked injection laser arrays," Appl. Phys. Lett. **44**, 293- 295 (1984).
24. E. Kapon, J. Katz, and A. Yariv, "Supermode analysis of phase-locked arrays of semiconductor lasers," Opt. Lett. **10**, 125-127 (1984).

1. Introduction

Phased laser arrays are often put forward as a means for achieving diffraction-limited output beams from a number of spatially separated coherent optical sources for applications including laser pumps, space communications, industrial welding and cutting, directed energy weapons, and laser induced nuclear fusion. These arrays are valuable alternatives wherever the required output beam power, brightness, and mode quality cannot be easily obtained from individual lasers. Agile beam steering and shaping are also potential benefits of coherent arrays, in analogy to phase-array radar antenna technology. Phase-locked diode lasers [1], CO_2 waveguide lasers [2], solid-state lasers [3], and fiber lasers [4] have been demonstrated, usually shortly after their corresponding individual lasers have been reported.

Although, kW-level single-core fiber lasers [5] have been achieved recently, phase-locked fiber laser arrays still attract increasing interest due to potential scaling to 10 kW or 100 kW fiber laser systems that can overcome power scaling constraints of single-element fiber lasers such as nonlinear effects, thermo-optic effects, output power saturation [6, 7], and optical damage [8]. Multicore fibers (MCFs), introduced by Scifres [9], can mitigate above-described restrictions on single-element/single-core lasers and provide a convenient and promising power scaling solution for compact fiber lasers. Phase-locked MCF lasers with different geometric configurations including 18 cores arranged in a ring array [10-12], 6 cores in a hexagonal array [13], 7 cores or 19 cores in a centered polygonal array [13-15], and antiguiding 5 cores in a linear array [16] have been demonstrated. To the best of our knowledge, there has been no report on the performance of phase-locked MCF lasers with multiple cores arranged in a rectangular array. Rectangular-array MCF lasers are expected to exhibit particular near-field distribution, far-field diffraction pattern, and splitting of propagation constants, which are different from those of other MCF arrays according to the array modal analysis using coupled-mode theory [17]. In this paper, we report on the characteristics of a phased-locked rectangular-array 12-core microstructured fiber laser and claim the first measurement of birefringence during in-phase mode operation of a MCF laser.

2. Multicore microstructured active fiber and its lasing characteristics

Microstructured fibers possess a specific cross-section that consists of an arrangement of air holes and rods running the entire length of the fiber. The microstructures not only provide a means of precisely controlling refractive index profiles [18], photonic bandgap [19], and dispersion properties [20]; they also provide the possibility of tailoring the polarization properties [21] of the fibers due to the large number of free design parameters including structure morphology, structure dimensions, hole and core profiles. Furthermore, by

#83153 - $15.00 USD Received 16 May 2007; revised 27 Jul 2007; accepted 30 Jul 2007; published 1 Aug 2007

integrating microstructures and multicore configurations, custom-shaped modes of fiber laser arrays can be devised [22]. Our 12-core microstructured fiber was fabricated by the method of stack-and-draw. The 12 cores are arranged in a 3 × 4 rectangular array, as shown in Fig. 1(a). The diameter of individual doped-cores is 8.5 μm and that of air holes is about 2 μm. The pitch of the microstructure is 8 μm and that results in the periods of the core array to be 14 μm and 16 μm in x and y directions, respectively. The refractive index of the core is 1.5698 and that of the cladding is 1.5690. This microstructure results in 12 individual cores with a numerical aperture of 0.16 and a modal field diameter of 11 μm. Therefore, the effective modal area of the whole structure is 1140 μm^2. The individual cores are co-doped with 1 wt% Er_2O_3 and 2 wt% Yb_2O_3, respectively. The MCF has an outer diameter of 125 μm which enables directly end-pumping by a multimode fiber coupled diode laser.

For pump powers below the lasing threshold individual cores emit only spontaneous emission and operate to a large extend separately, resulting in nearly identical intensities of individual cores as shown in Fig. 1(b). In contrast, when pumping the MCF above the lasing threshold, individual cores do not operate separately any more. In this case, the cores interact due to evanescent coupling between neighboring cores, and the intensity of individual cores has an uneven distribution which reflects a combined near-field pattern of several lasing supermodes, shown in Fig. 1(c).

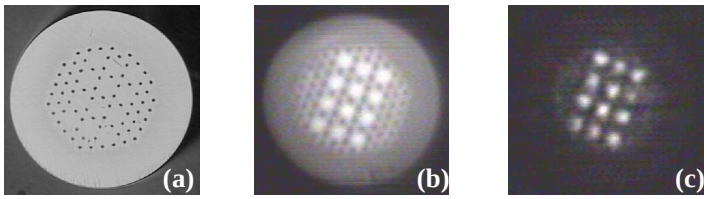

Fig. 1. Microscopic images of the output facet of a 12-core microstructured Er/Yb co-doped phosphate fiber laser when (a) without pumping, (b) spontaneous emission, and (c) stimulated emission.

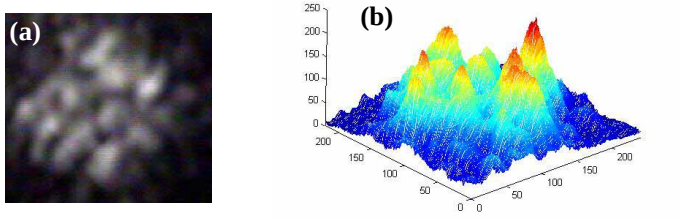

Fig. 2. Far-field intensity distribution of a free-running 12-core microstructured Er/Yb co-doped phosphate fiber laser. (a) Pattern image, (b) 3-D description of (a).

According to the modal analysis of laser arrays [17, 23, 24], in a laser array with N elements, the interaction among the elements results in the formation of a set of N supermodes, each being a linear superposition of the individual cores modes. Therefore, there exist 12 supermodes (neglecting polarization effects) for the 12-core microstructured fiber laser. Without any modal selection mechanism, however, supermodes with higher gain and lower cavity round trip loss are most likely to emit in a free-running MCF laser. The typical far-field pattern of a free-running 12-core microstructured fiber laser is shown in Fig. 2. The far-field distribution is characterized by multiple peaks, in striking contrast to an incoherent addition of 12 individual lasers. The pattern indicates the oscillation of several supermodes, resulting in wide diffraction and a beam profile that is of little practical use.

#83153 - $15.00 USD Received 16 May 2007; revised 27 Jul 2007; accepted 30 Jul 2007; published 1 Aug 2007

3. Experiments and analyses of in-phase supermode operation

The fundamental supermode, corresponding to adjacent cores emitting in phase (therefore also called in-phase supermode), is the most desired emission mode of a laser array, because its far-field beam pattern is single-lobed centered around zero degree. Laser operation in the fundamental supermode within tailored external cavities can be enforced using spatial filters [10, 11], output couplers [13, 14], and waveguides [12, 15] by utilizing the fact that field distributions and diffractive losses are different among the supermodes. In our experiment, an output coupler with transmission of 54% at laser wavelength was placed after the MCF and modal selection was realized by tuning the output coupler. The experiment setup for investigating the performance of the 12-core microstructured fiber laser with in-phase oscillation is schematically depicted in Fig. 3. A multimode pump delivery fiber, with a dichroic coating (HR @ 1535 nm and HT @ 974 nm) deposited on its facet, was butt-coupled to the MCF. The near-field and far-field patterns of the MCF laser were recorded by an infrared CCD camera.

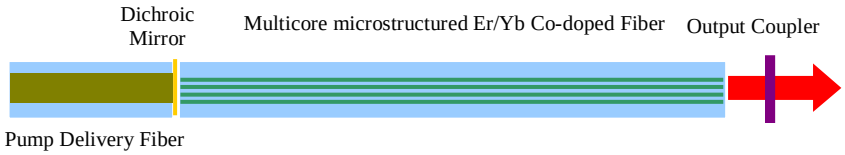

Fig. 3. Experimental setup for the phase-locked 12-core microstructured Er/Yb co-doped phosphate fiber laser.

Similar to previous analyses of diode laser arrays, we can use the coupled-mode theory [17, 23, 24] to analyze the performance of the 12-core rectangular-array MCF laser. Under the assumption that all individual cores are identical, the near-field distribution of the fundamental in-phase supermode of a 3 × 4 laser array can be expressed by

$$E_{11}^{X,Y}(x,y,z)=\sum_{l=1}^{3}\sum_{m=1}^{4}\sin\left(\frac{l\pi}{4}\right)\sin\left(\frac{m\pi}{5}\right)E_{00}^{X,Y}(x-x_{lm},y-y_{lm})e^{i\gamma_{11}^{X,Y}z}, \tag{1}$$

where X and Y represent the two orthogonal polarization fields, l and m are the core unit indices, $E_{00}^{X,Y}(x\text{-}x_{lm}, y\text{-}y_{lm})$ is the field distribution of individual cores, and $\gamma_{11}^{X,Y}$ is the polarization dependent propagation constant of the fundamental supermode, which can be written as

$$\gamma_{11}^{X,Y}=\beta^{X,Y}+\kappa_x^{X,Y}\cos\left(\frac{\pi}{4}\right)+\kappa_y^{X,Y}\cos\left(\frac{\pi}{5}\right), \tag{2}$$

where $\beta^{X,Y}$ is the propagation constant of the individual core; $\kappa_x^{X,Y}$ and $\kappa_y^{X,Y}$ are the coupling constants between two neighboring cores in x and y directions, respectively. The far-field intensity distribution of the fundamental supermode can be written as

$$I_{11}^{X,Y}(\theta,\phi)=\left\{\frac{\sin[3(S_x+\pi/4)/2]}{\sin[(S_x+\pi/4)/2]}+\frac{\sin[3(S_x-\pi/4)/2]}{\sin[(S_x-\pi/4)/2]}\right\}^2 \times\left\{\frac{\sin[4(S_y+\pi/5)/2]}{\sin[(S_y+\pi/5)/2]}+\frac{\sin[4(S_y-\pi/5)/2]}{\sin[(S_y-\pi/5)/2]}\right\}^2 I_{00}^{X,Y}(\theta,\phi), \tag{3}$$

where $S_x=k_0p_x\sin\theta\cos\phi$, $S_y=k_0p_y\sin\theta\sin\phi$, p_x and p_y are the periods of the core array in x and y directions, respectively, and $I_{00}^{X,Y}(\theta,\phi)$ is the far-field intensity distribution of an individual core.

The near-field distribution of the phased MCF laser, shown in Fig. 4(b), was recorded by imaging the output facet of the MCF to the CCD camera with a magnifying lens. The distributions of two selected cross-sections along x and y direction [along the lines in Fig. 4(b)] is shown in Figs. 4(a) and (c), respectively. The experimentally obtained distributions are in good agreement with theoretical results for the in-phase supermode obtained from Eq. (1).

#83153 - $15.00 USD Received 16 May 2007; revised 27 Jul 2007; accepted 30 Jul 2007; published 1 Aug 2007

The far-field pattern was recorded on a screen 11 cm away from the output facet and its distributions are shown in Figs. 5(a) – (c). The angle spreads, which are taken the full width at half maximum (FWHW), along x and y directions are 36 and 27 mrad, respectively. Optical spectra were also measured to further characterize free-running vs. in-phase supermode operation. As shown in Fig. 6, in-phase supermode operation gives a narrower emission spectrum than free-running operation does. The output power during in-phase supermode operation was also measured as a function of pump power. The slope efficiency was about 10% and the maximum output was 2.6 W.

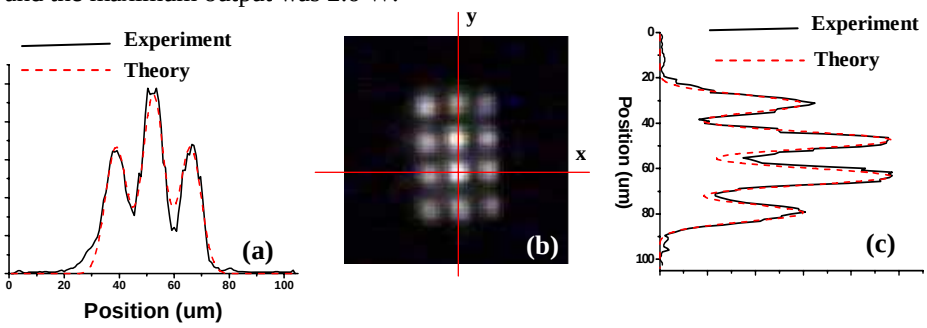

Fig. 4. Near-field distribution of the phase-locked 12-core microstructured Er/Yb co-doped phosphate fiber laser. (a) Profile along x direction, (b) near-field image, (c) profile along y direction.

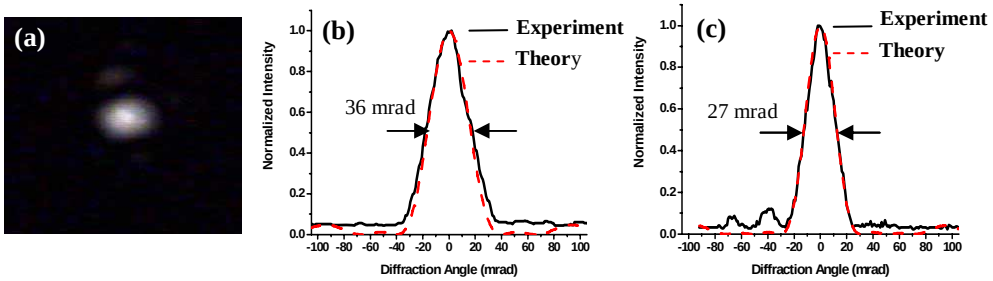

Fig. 5. Far-field intensity distribution of the phase-locked 12-core microstructured Er/Yb co-doped phosphate fiber laser. (a) Far-field pattern, (b) diffraction profile along x direction, (c) diffraction profile along y direction.

To evaluate the polarization mode splitting, the radio frequency (RF) spectrum of the output, i.e., beating signals generated by interference between various longitudinal modes, has been measured. Longitudinal mode beating (LMB) signals, generated by interference between modes of the same polarization field, tell us the free spectral range $\Delta\nu_{LMB} = c/(2n_{eff}L)$, while polarization mode beating (PMB) signals, generated by interference between modes of two polarization fields, can tell us the polarization mode splitting in frequency $\Delta\nu_{PMB} \approx c\Delta n_{eff}/(\lambda n_{eff})$. All RF signals can be recorded, as shown in Fig. 7, with a RF spectrum analyzer. To note, the 744 MHz signal, paired with the zero frequency component, corresponds to $\Delta\nu_{LMB}$; and the signals at 120, 624, and 864 MHz are generated by PMB. This indicates that the in-phase mode is split into two non-degenerate polarization states and $\Delta\nu_{PMB}$ is 120 MHz. The corresponding birefringence Δn_{eff} can thus be obtained by $\Delta n_{eff} = \Delta\nu_{PMB}\lambda/(\Delta\nu_{LMB}L)$. The effective group index birefringence is $\sim 10^{-6}$ and the corresponding propagation constant birefringence, namely, $\Delta\gamma = 2\pi\Delta n_{eff}/\lambda$, is $\sim 4 \times 10^{-6}$ 1/μm. However, according to Eq. 2, the polarization mode discrimination can be caused by polarization dependence of either the propagation constant β of individual cores or the coupling coefficient κ_x and κ_y. Although a birefringence value is measured here, it remains to be identified whether it is induced by the

#83153 - $15.00 USD Received 16 May 2007; revised 27 Jul 2007; accepted 30 Jul 2007; published 1 Aug 2007

birefringence in individual cores or by the asymmetry of the rectangular array and the microstructured fiber cross-section.

Though in-phase operation has been demonstrated in different MCF lasers and amplifiers [10-16], we are not aware of any similar investigation related to the polarization properties of MCFs. Polarization and birefringence are, however, very important for many applications where polarization maintenance or single polarization is required within a multicore power-scaling approach. Our first direct measurement of birefringent in-phase operation of a MCF laser inspires an impetus to tailor the polarization properties of future multicore fiber lasers and amplifiers. A tailored multicore pattern can also be combined with more traditional approaches including asymmetric stresses in the cladding or elliptical individual cores [21] to further enhanced the birefringence of MCFs.

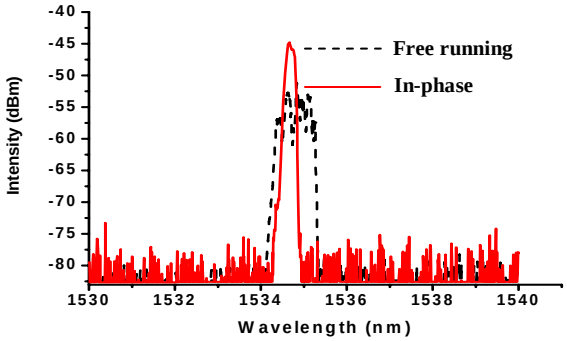

Fig. 6. Optical spectra of free-running (dashed line) and in-phase operation (solid line) of the 12-core microstructured Er/Yb co-doped phosphate fiber laser.

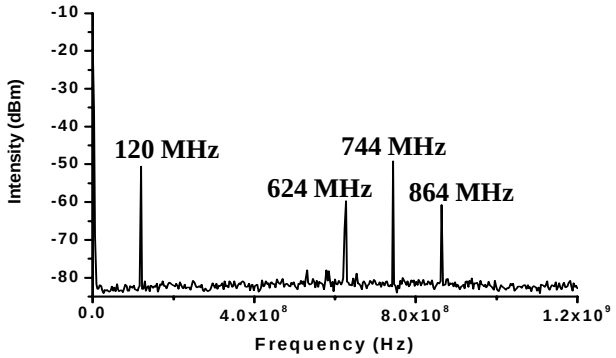

Fig. 7. RF spectrum of the LMB and PMB signals showing two non-degenerated, polarized in-phase supermodes emitted by the 12-core microstructured Er/Yb phosphate fiber laser.

4. Conclusion

We have analyzed free-running and in-phase operation of a 12-core rectangular-array microstructured fiber laser. The agreement between experimental results and theoretical calculations confirmed the in-phase operation of the MCF laser. Through fiber and cavity design we can tailor the beam profile and emission pattern of the MCF laser. Our observed birefringence of the in-phase supermode indicates the possibility of polarization maintaining MCF and single polarization, high-power MCF lasers and amplifiers.

Acknowledgments

The authors would like to thank Y. Merzlyak for technical support. This work is supported by the U. S. Air Force Office of Scientific Research through MRI program, F49620-02-1-0380, National Science Foundation grants 0335101 and 0725479, and the State of Arizona TRIF Photonics Initiative.

#83153 - $15.00 USD Received 16 May 2007; revised 27 Jul 2007; accepted 30 Jul 2007; published 1 Aug 2007